

See discussions, stats, and author profiles for this publication at: <https://www.researchgate.net/publication/230559273>

Synthesis and Laser Immobilization Onto Solid Substrates of CdSe/ZnS Core–Shell Quantum Dots

ARTICLE in THE JOURNAL OF PHYSICAL CHEMISTRY C · AUGUST 2011

Impact Factor: 4.77 · DOI: 10.1021/jp203051b

CITATIONS

10

READS

29

8 AUTHORS, INCLUDING:



[Angel Pérez Del Pino](#)

Materials Science Institute of Barcelona

73 PUBLICATIONS 1,458 CITATIONS

[SEE PROFILE](#)



[Ana Sofia Miguel](#)

Instituto de Tecnología Química e Biológica ...

10 PUBLICATIONS 58 CITATIONS

[SEE PROFILE](#)



[Christopher D. Maycock](#)

New University of Lisbon

108 PUBLICATIONS 1,422 CITATIONS

[SEE PROFILE](#)



[Abel G Oliva](#)

New University of Lisbon

54 PUBLICATIONS 486 CITATIONS

[SEE PROFILE](#)

Synthesis and Laser Immobilization onto Solid Substrates of CdSe/ZnS Core–Shell Quantum Dots

E. György,^{*,†,‡} A. Pérez del Pino,[§] J. Roqueta,[†] B. Ballesteros,[†] A. S. Miguel,^{||} C. D. Maycock,^{||,#} and A. G. Oliva^{||}

^{*}Centre d'Investigació en Nanociència i Nanotecnologia, Institut Català de Nanotecnologia, Consejo Superior de Investigaciones Científicas, (CIN2, ICN-CSIC), Campus UAB, 08193 Bellaterra, Spain

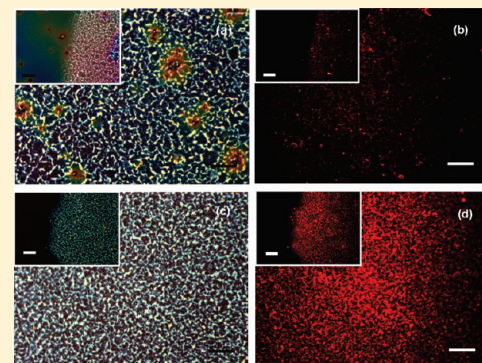
[†]National Institute for Lasers, Plasma and Radiation Physics, P.O. Box MG 36, 76900 Bucharest V, Romania

[§]Instituto de Ciencia de Materiales de Barcelona, Consejo Superior de Investigaciones Científicas (ICMAB-CSIC), Campus UAB, 08193 Bellaterra, Spain

^{||}Instituto de Tecnología Química e Biológica, Universidade Nova de Lisboa, 2781-901 Oeiras, Portugal

[#]Departamento de Química e Bioquímica, Faculdade de Ciências, Universidade de Lisboa, 1749-016 Lisboa, Portugal

ABSTRACT: CdSe/ZnS core–shell quantum dots (QDs) have been immobilized by ultraviolet matrix-assisted pulsed laser evaporation (UV-MAPLE) onto SiO₂ glass substrates covered by silica thin films. The silica thin films were deposited by the sol–gel method. An UV KrF* ($\lambda = 248$ nm, $\tau_{\text{fwhm}} \approx 25$ ns) excimer laser source was used for the laser immobilization experiments. Toluene was chosen as solvent material for the preparation of the composite MAPLE targets. The surface morphology and growth mode of the deposited structures were investigated by optical and atomic force microscopy in acoustic (dynamic) configuration. The crystalline structure and chemical composition of the base material used for the preparation of the MAPLE targets as well as the laser transferred QDs were studied by transmission electron microscopy and energy dispersive X-ray spectroscopy. The functional properties of the immobilized QDs were studied by fluorescence microscopy. The immobilized materials form self-organized 2D arrays constituted by complex CdSe/ZnS core–shell QDs preserving the functional properties of the base material used for the preparation of the MAPLE targets.



1. INTRODUCTION

Semiconductor quantum dots (QD) are nanocrystals composed of hundreds to up to a few thousand atoms. These nanostructures can be prepared in a variety of compositions, and shapes as nearly spherical,¹ elongated nanorods,² or crystals with more complex shapes such as tetrapods.³ The small size of these systems leads to a quantum confinement effect, resulting in a strong modification of their band structure. In these conditions, effects such as an expansion of the band gap, the quantization of the energy levels to discrete values and the strong enhancement of the Coulomb interaction between the charge carriers take place. Such phenomena have a great effect in the e-h dynamical behavior, arising exciting mechanisms such as the direct generation of multiexcitons by single photons (carrier multiplication).⁴

As known, the physical properties of the QDs are size dependent.^{5,6} Thus, remarkable electronic and photonic characteristics can be tuned by simply controlling their shape and size, adding up significant functionality in applications as biological labeling, nonlinear optics, or photovoltaics technology.^{7,8} A step forward consists in overcoating such QDs with a shell of a second semiconductor, resulting in core–shell systems that exhibit novel properties as compared to simple dots.⁹ Overcoating the nanocrystals with higher band gap inorganic materials has been

found to improve the photoluminescence quantum yields by passivating surface nonradiative recombination sites.^{10,11} In addition, nanoparticles passivated with inorganic shells are more robust than those passivated with organic materials and withstand more severe processing conditions when incorporated into solid state structures. Besides, by the appropriate choice of the core and shell materials, it is possible to adjust the emission wavelength in a larger spectral range than with both materials alone.^{12,13} These features make them promising besides emitters for quantum information, also for biological labeling,^{14,15} design of devices such as thin film LEDs,^{16–18} or nanocrystal quantum dot lasers.^{19–21}

CdSe/ZnS core–shell QDs are usually deposited on solid substrates from colloidal solutions by conventional methods as drop casting or spin coating. These techniques are rather simple and cost-effective. However, they do not guarantee an accurate control over the amount of the immobilized material and its surface uniformity. In addition, conventional methods are not suitable for multilayer structures growth since they imply

Received: April 1, 2011

Revised: June 30, 2011

Published: July 01, 2011

repeated use of solvents. Laser technologies could represent an alternative solution for these drawbacks: the amount of evaporated and deposited material on the substrate surface can be controlled through the number and/or irradiance of the laser pulses, offering high reproducibility and versatility for multilayer synthesis. However, immobilization of nanoparticles with a narrow size distribution by conventional pulsed laser deposition technique can be a difficult task. Usually the deposited nanoparticles have a broad size distribution range and often form aggregates with dimensions in the micrometer range. An additional problem in the case of multicomponent materials represents the selective evaporation of elements making difficult to reproduce structures with identical chemical composition as the base materials used as targets submitted to laser irradiation.

Matrix-assisted pulsed laser evaporation (MAPLE) is a laser-based deposition technique developed more recently, mostly for organic and bio-organic materials processing.²² The material to be immobilized on a solid substrate surface is diluted in a laser-absorbing solvent. After the solution is frozen in liquid nitrogen it is submitted to laser radiation. The laser energy is mainly absorbed by the solvent which is vaporized and transports the material of interest toward the substrate placed in front of the target ensuring a gentle transfer mechanism. Besides organic species, some recent works have demonstrated the possibility to transfer TiO₂ and SnO₂²³ or carbon nanoparticles²⁴ by ultraviolet (UV)-MAPLE as well as CdSe QDs²⁵ by resonant infrared (RIR)-MAPLE techniques.

We report in this paper the creation of self-organized 2D arrays constituted by complex CdSe/ZnS core–shell QDs immobilized on solid substrates by UV-MAPLE technique. The networklike structures synthesis can be controlled by the incident laser fluence value. The formation of a photonic band gap due to the periodically changing refractive index can be used for future photonic applications implying guided light propagation or enhanced spontaneous emission.

2. EXPERIMENTAL SECTION

2.1. Synthesis of Core–Shell CdSe/ZnS QDs. The chemical reagents and solvents used for the CdSe/ZnS QDs synthesis were obtained from Sigma-Aldrich and Fluka. Air-sensitive materials were handled in a Braun MB150-GI glovebox under dry argon atmosphere. All solvents were spectrophotometric grade. Trioctylphosphine oxide (TOPO)/hexadecylamine (HDA) capped CdSe QDs were synthesized using standard procedures,²⁶ generating nanocrystals with the first absorption peak around 560–570 nm and diameters of 3.6–4.5 nm. The growth of the ZnS shell coating is based on SILAR method²⁷ which consists of injections of Zn and S precursors to the solution containing CdSe nanocrystals suspended in octadecene (ODE)/HDA. 0.1 M solutions of ZnO in ODE/oleic acid and S in ODE were used. For each monolayer shell growth, a calculated amount of these solutions were simultaneously injected via syringe into the dot suspension at 245 °C using standard gas-free conditions. A period of 10 min between each addition was left for the reaction to be complete. The CdSe cores were covered with 5 ZnS monolayers, which took about 1 h and 30 min. Then, the solution was kept for another 30 min at 260 °C and finally cooled down to room temperature. After extraction with methanol, centrifugation, and decantation, the particles were dispersed in chloroform and capped with a layer of TOPO/HDA.

2.2. Laser Immobilization of CdSe/ZnS QDs on SiO₂ Glass Substrates. The laser immobilization experiments were performed inside a stainless steel deposition chamber. A pulsed UV KrF* ($\lambda = 248$ nm, $\tau_{\text{fwhm}} \approx 25$ ns, $\nu = 10$ Hz) COMPExPro 205 Lambda Physik excimer laser source was used for the irradiations. Prior to each experiment, the irradiation chamber was evacuated down to a residual pressure of 10^{-3} Pa. This pressure value was maintained during the experiments.

For the preparation of the composite MAPLE targets 2.5 μg CdSe/ZnS core–shell QDs were added to 3 mL of toluene. The obtained solutions were introduced into a special double wall target holder and flash-frozen at –190 °C circulating liquid nitrogen inside the holder walls. The targets were kept frozen during the irradiation experiments. The complete MAPLE workstation was purchased from SURFACE.

To avoid significant morphological changes upon irradiation, the laser beam scanned the targets' surface at a constant velocity of 2 mm/s. The irradiated XY surface area was $1 \times 1 \text{ cm}^2$. The angle between the laser beam and the target surface was chosen of 45°. The number of subsequent laser pulses applied for the deposition of the nanostructures was 5×10^3 . The laser pulses succeeded each other with a repetition rate of 10 Hz. The laser fluence value incident on the target's surface was fixed at 0.1 or 0.2 J/cm².

Silica films coated on SiO₂ glass substrates were placed parallel to the target at a separation distance of 5 cm. The silica films were deposited by sol gel technique based on the method described previously.^{28,29} The solution was composed by two types of precursors, tetraethyl orthosilicate (TEOS) and methyltriethoxysilane (MTES). The TEOS/MTES molar ratio was 1:1. The films were deposited by dip-coating onto 6.5 mm × 50 mm SiO₂ glass substrates in a two step process with 1 min interval between them. Drying was performed at room temperature for 24 h followed by thermal treatment at 70 °C for 24 h. For the described experimental conditions a film porosity of 26% was estimated from nitrogen absorption isotherms, with a pore size ranging between 2 and 10 nm.²⁹ Prior to introduction inside the irradiation enclosure the substrates were carefully cleaned in ultrasonic bath in acetone. During the laser irradiations the substrates were kept at room temperature.

The CdSe/ZnS core shell QDs were investigated by transmission electron microscopy (TEM). A JEOL 2011 transmission electron microscope operated at an acceleration voltage of 200 kV was used for observing the CdSe/ZnS QDs. The samples were purified by acetone precipitation from their chloroform or hexane solutions. The laser immobilized QDs were prepared for TEM analysis by placing a droplet of milli-Q water on the deposited nanostructures with a subsequent mild stirring to suspend the QDs. The droplet was then transferred with a pipet onto a carbon-coated copper grid and left to evaporate. Energy dispersive X-ray spectroscopy (EDX) analyses were carried out using an Oxford Instruments EDX detector controlled by INCA software. Quantum yields (QY) measurements were performed with the aid of a SPEX-Fluorolog fluorometer spectrometer relative to Rhodamine 6G dye, at 530 nm excitation wavelength. Solutions of QDs in chloroform and dye in ethanol were optically matched at the excitation wavelength. Fluorescence spectra of solutions containing QDs and dye were taken under identical spectrometer conditions. To calculate QY the optical density at the peak was kept below 0.05, and the integrated intensities of the emission spectra were corrected for differences in index of refraction and concentration. The hydrodynamic

diameter (HD) of the synthesised CdSe/ZnS core–shell QDs was measured by dynamic light scattering analysis using a Nano series dynamic light scatterer from Malvern. The samples were measured in CHCl_3 with QD concentrations between 0.06 and $0.30 \mu\text{M}$ and filtered through a $0.2 \mu\text{m}$ filter before analysis. The surface morphology and growth mode of the deposited nanostructures were investigated by atomic force microscopy (AFM) by intermittent contact (dynamic) configuration with a S100 AFM/SPM apparatus from Agilent Technologies. The AFM measurements were studied with MountainsMap software from Digital Surf. Fluorescence optical images were acquired using a Carl Zeiss Axio Observer Z1 inverted microscope equipped with a motorized XY stage. A 100-W Hg lamp was used as excitation light source. Microscope images were acquired with an AxioCamHR digital CCD Color Camera and image capture and exposure times were controlled using Axio Vision Rel 4.6 software.

3. RESULTS AND DISCUSSIONS

The synthesized CdSe/ZnS core–shell QDs were analyzed by TEM (Figure 1). As can be observed in the higher resolution TEM image (Figure 1b), the QDs have a narrow size distribution, with dimensions between 4 and 6 nm. High-resolution TEM (HRTEM) investigations showed that the particles have two different crystalline structures. The measured interplanar distances correspond to the ZnS hexagonal wurtzite as well as ZnS cubic zinc-blende phases. No significant difference can be observed as concerns the crystalline structure between the QDs immobilized with different laser fluence values as well as the nonirradiated base material (Figure 2). The interplanar distances correspond to the bulk ZnS hexagonal wurtzite and ZnS cubic zinc-blende crystalline phases. These measured bulk interplanar distances can be explained by the high ~ 5 ZnS monolayers shell coverage, since it has been reported that at

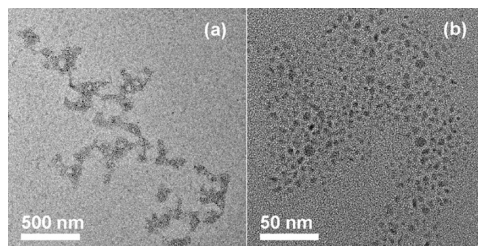


Figure 1. TEM images of CdSe/ZnS core shell QDs deposited on SiO_2 glass substrates covered by silica sol gel deposited film at $0.1 \text{ J}/\text{cm}^2$ laser fluence.

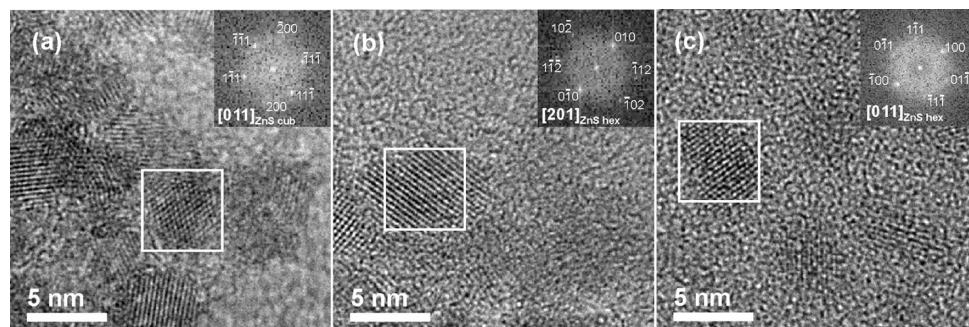


Figure 2. HRTEM images and fast Fourier transform patterns of (a) reference drop-cast sample and CdSe/ZnS core shell QDs deposited on SiO_2 glass substrates covered by silica sol gel deposited film at (b) 0.2 and (c) $0.1 \text{ J}/\text{cm}^2$ laser fluence.

coverage higher than ~ 2 monolayers ZnS shells grow with the bulk ZnS lattice parameter, with incoherence between the CdSe core and the ZnS shell.¹¹ As in our case, TEM micrographs correspond to the ZnS structure and the growth of the thick ZnS overlayer was described as epitaxial but incoherent.¹¹ The EDX data confirms that the laser deposited nanostructures are composed by CdSe and ZnS (Figure 3).

For the QY measurements the integrated intensity areas of the fluorescence emission spectra for both solutions, one containing QDs and the other dye, were corrected for differences in index of refraction and concentration. The optical absorbance of QDs containing solution at the excitation wavelength was about 0.05. The QY was calculated by the relative method³⁰ according to the equation

$$\text{QY}_{\text{QD}} = \text{QY}_{\text{dye}} (A_{\text{dye}}/A_{\text{QD}}) (E_{\text{QD}}/E_{\text{dye}}) (n_{\text{QDsolvent}})^2 / (n_{\text{dyesolvent}})^2$$

Where QY_{dye} stands for the QY of the solution containing the Rhodamine 6G dye, A the absorbance of the solutions, E the corrected intensity areas, and n the average refractive index of the solutions. A QY of 0.12 was estimated. The relatively low QY value could be associated with the high coverage of QDs, approximately 5 ZnS monolayers. It was reported that the QY begins to decrease as the surface coverage exceeds approximately a completed ZnS shelling.^{11,12,31} This behavior was attributed to the effect of strain created at the interface due to the 12% lattice mismatch between CdSe and ZnS leading to an incoherent epitaxial mechanism for the growth of the ZnS shell at high coverage, as suggested also by our HRTEM results. The relaxation of the crystallographic structure should be associated with formation of structural defects, dislocations, and grain boundaries and creation of sources for nonradiative recombination sites in the ZnS shell.¹¹

Figure 4 shows the tilted AFM image (a) and surface profile (b) across the line marked in the AFM image of silica films deposited by sol gel technique on SiO_2 glass substrate. The formation of dome-shaped structures of the films surface can be observed, with an average in-plane diameter of about $0.5\text{--}1 \mu\text{m}$ and height around 30 nm. The density of these structures is about $0.1 \mu\text{m}^{-2}$. A root-mean-square (rms) roughness of 1.5 nm was measured. We would like to note that the porous structure of the layers can not be observed due to the small size of the pores, smaller or similar to the AFM tip diameter of 10 nm. Then, the surface roughness is underestimated, including also the contribution of the AFM tip.

Figure 5 shows the tilted (a, b, d, e) AFM images as well as surface profiles (c, f) across the line marked in the AFM images of

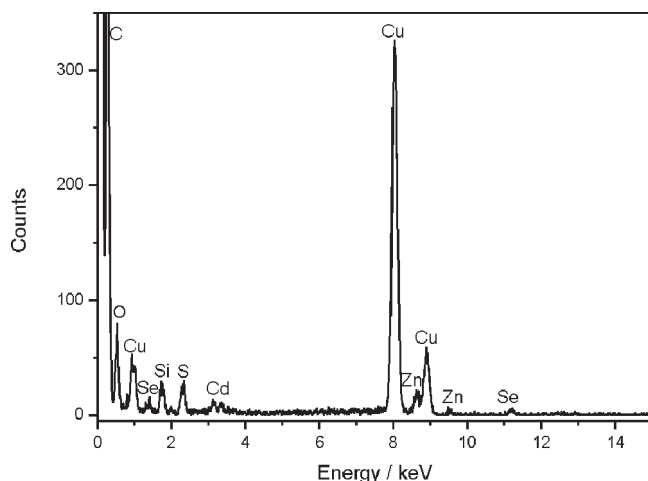


Figure 3. EDX spectrum of CdSe/ZnS core shell QDs deposited on SiO_2 glass substrates covered by silica sol gel deposited film at 0.1 J/cm^2 laser fluence.

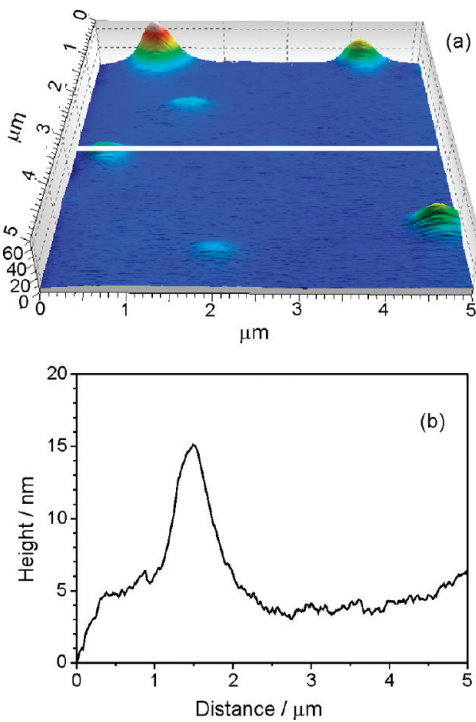


Figure 4. Tilted AFM micrograph and surface profile across the line marked in the AFM micrograph of sol gel deposited silica film on SiO_2 glass substrates.

CdSe/ZnS core–shell nanoparticles immobilized on SiO_2 glass substrates coated with silica films, at incident laser fluence values of 0.2 (a–c) and 0.1 J/cm^2 (d–f). The particulates present on the surface of films deposited at both laser fluence values have a quite homogeneous size distribution. As can be observed, the deposited material consists of tens of nanometer sized clusters. However, at 0.2 J/cm^2 laser fluence the deposition is not continuous over the substrate surface forming an interconnected line-structure (marked in Figure 5a). At higher magnification the individual particles can be clearly distinguished (Figure 5 b).

With the decrease of the laser fluence the deposited films surface is characterized by a more uniform morphology, constituted by tens of nanometer sized particulates (parts d and e of Figure 5).

The efficiency and homogeneity of the QDs attachment is superior on the silica buffer layer related to the nontreated glass slide surface (data not shown). This could be due to the porosity of the surface and the presence of dome-shaped structures providing a higher specific surface area and therefore a larger available area for QDs attachment as compared to the completely flat glass substrate. Moreover, the porous silica structure can be broken locally by the laser transferred particles. Note that at higher magnification the particles seem to be embedded in the silica matrix (parts b and e of Figure 5). In addition, it was reported that multivalent hydrophobic interactions provide a strong driving force for efficient immobilization of TOPO surfactant-coated QDs in silica nanopores.³² A further advantage of the silica film is that allows for the utilization of different support materials (glass, fiber optics, polymeric or plastic, etc.) keeping similar characteristics as regards surface topography for the QDs deposition.

The optical micrographs (parts a and b of Figure 6) of immobilized CdSe/ZnS core–shell nanoparticles evidence the formation of a long-range self-organized networklike morphology. The network is constituted by interconnected lines as observed also by AFM (see Figure 5a) composed by CdSe/ZnS QDs with transversal dimensions reaching about one micrometer and lengths of several micrometers. Figure 5b shows a detail of one of these lines constituted by tens of nm sized clusters. The density of the lines increases with the decrease of the laser fluence, resulting in a percolated structure.

Figure 7 shows the optical microscope (a) and the fluorescence (b) images corresponding to the same surface area of a positive reference (blank) sample prepared by the deposition onto SiO_2 glass substrate of a drop from the solution, $2.5 \mu\text{g}$ of CdSe/ZnS core shell QDs in 3 mL toluene, used for the frozen composite targets preparation in the MAPLE experiments. The observed orange fluorescence (Figure 7b) is characteristic for the CdSe/ZnS QDs using UV light for excitation.

The optical microscopy images and the fluorescence patterns corresponding to the same surface area of the deposited QDs on the SiO_2 glass substrates coated by silica films are presented in Figure 8. The insets belong to the edge of the depositions, the border between the substrate surface and the laser transferred QDs. The fluorescence image corresponding to the sample obtained with 0.1 J/cm^2 (Figure 8d) is more intense as compared to that of the QDs immobilized using higher, 0.2 J/cm^2 laser fluence (Figure 8b) and reproduces the characteristic organized, networklike surface morphology. On the other hand, the intensity of the fluorescence patterns of the laser immobilized QDs can not be compared to that of the reference drop-cast sample (Figure 7b). A direct comparison would be possible only if the quantity of the laser evaporated QDs would be equal to the quantity of the QDs deposited by drop-casting. The few randomly distributed large micrometer sized particulates visible also in parts a and b of Figure 6 are the most probably characteristic for the substrate surface morphology since they are present on the uncovered substrate areas as well (see inset of Figure 8a).

The QDs are transported to the substrate surface the most probably by the solvent vapor. The laser pulses incident onto the frozen target cause melting of the composite target followed by the vaporisation of the liquid solvent. We would like to note that we chose toluene as solvent for the frozen composite targets

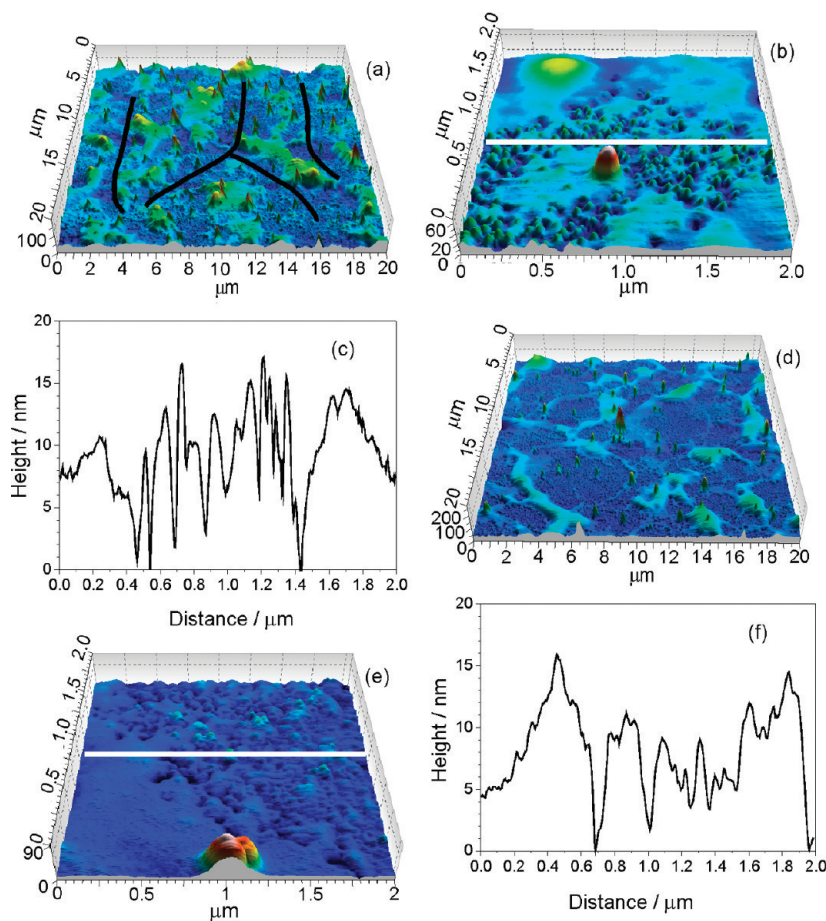


Figure 5. Tilted AFM micrographs (a, b, d, e) as well as surface profiles (c, f) across the lines marked in the AFM micrographs of CdSe/ZnS core shell QDs thin films obtained on SiO_2 glass substrates covered by silica sol gel deposited film at (a, b, c) 0.2 and (d, e, f) 0.1 J/cm^2 laser fluence.

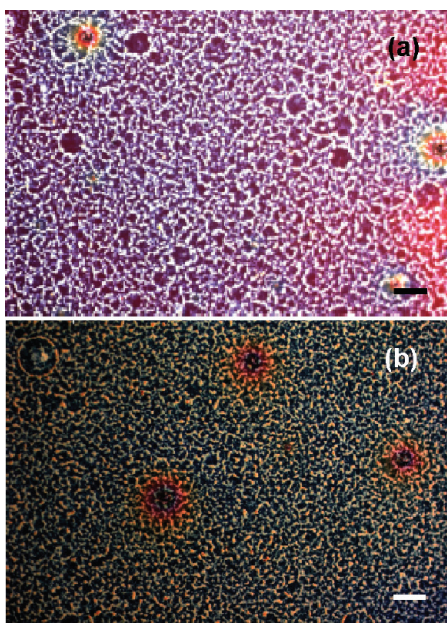


Figure 6. Optical microscopy images of CdSe/ZnS core shell nanostuctures obtained on SiO_2 glass substrates covered by silica sol gel deposited film at 0.2 (a) and 0.1 J/cm^2 (b) laser fluence. Scale bars correspond to 20 μm .

preparations due to its highly absorption at the wavelength of the incident laser radiation. This is the typical situation in MAPLE experiments, where the solvents are highly absorbing at the incident laser wavelength in order to ensure a protection for the material to be irradiated and transferred to the substrate surface.

On the other hand, the laser radiation is also absorbed by the QDs. The threshold laser fluences necessary for ablation and plasma ignition upon KrF* excimer laser irradiation of CdSe and ZnS with a pulse width of 14 ns were estimated to be 0.1 and 1.3 J/cm^2 for CdSe and ZnS, respectively. These laser fluence values correspond to incident laser irradiances of 7.1 and 92.8 MW/ cm^2 , respectively.³³ Moreover, it was found that due to the low sublimation temperature of ZnS, the sublimation process is responsible for the onset of ablation, before the material reaches its melting temperature.³⁴ Theoretical calculations showed that a threshold laser irradiance value of 16.6 MW/ cm^2 is sufficient to reach the sublimation temperature on the surface of ZnS:Mn thin films.³⁵ We would like to note that the 0.2 J/cm^2 laser fluence used in our experiments corresponds to an irradiance of 8 MW/ cm^2 , well below the calculated sublimation threshold value. However, the thermal diffusion length in ZnS for 25-ns laser pulses can be estimated at around 900 nm.³⁶ As a consequence, the ablation process in case of the only 5 monolayer thick ZnS shells is governed by the CdSe cores, the incident laser irradiance being at the limit of the estimated plasma ignition threshold.³³ Then, part of the irradiated QDs especially those situated in the

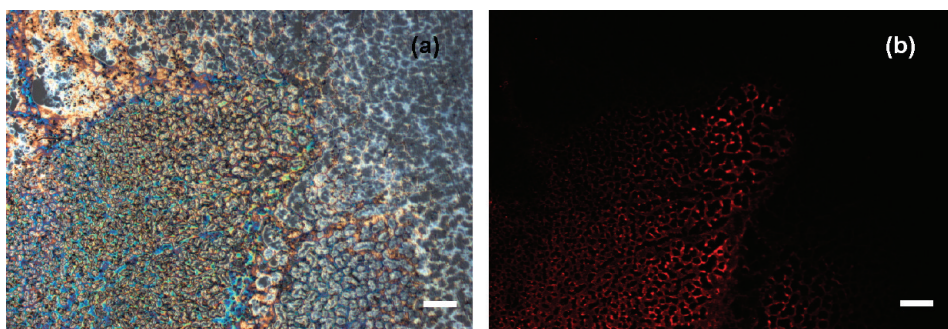


Figure 7. Optical microscopy (a) and fluorescence (b) images corresponding to the same surface area of positive reference (blank) sample prepared by the deposition onto SiO_2 glass substrate of a drop from the solution, 2.5 μg of CdSe/ZnS core shell QDs in 3 mL toluene, used as targets in the MAPLE experiments. Scale bars correspond to 20 μm .

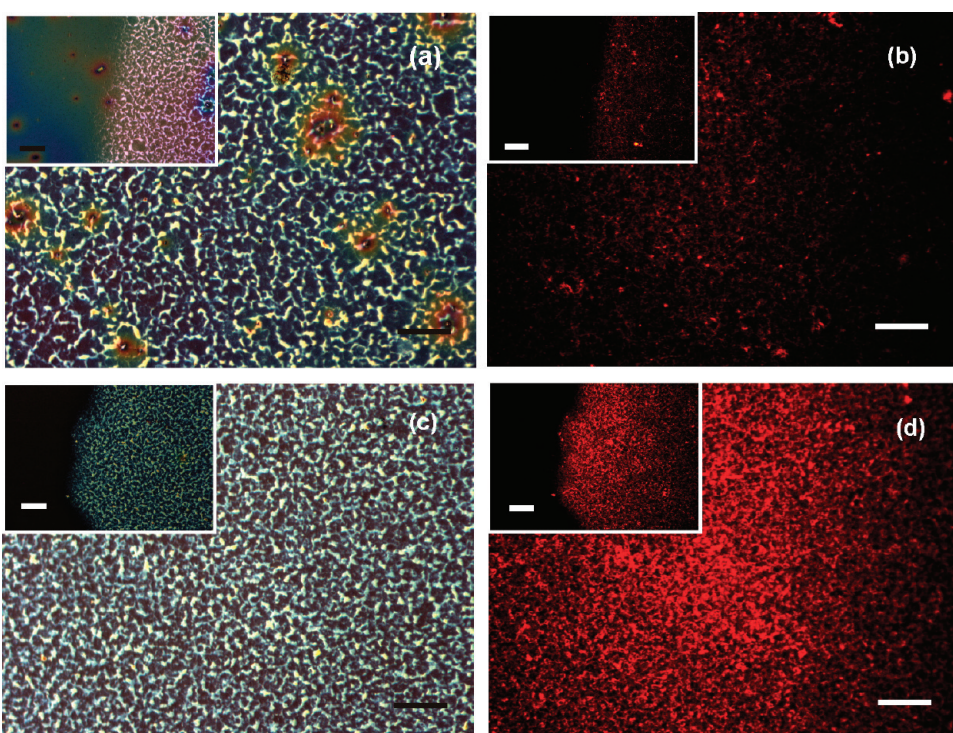


Figure 8. Optical microscopy (a, c) and fluorescence (b, d) images corresponding to the same surface area of CdSe/ZnS core shell nanostructures obtained on SiO_2 glass substrates covered by silica sol gel deposited film at 0.2 (a, b) and 0.1 J/cm^2 (c, d) laser fluence. The insets belong to the border between the substrate and CdSe/ZnS QDs thin films. Scale bars correspond to 20 μm .

outmost surface layer of the frozen composite target could be damaged. However, the solvent vapor can carry QDs toward the substrate surface from deeper zones, where the temperature just surpasses the evaporation temperature of toluene.

Conversely, the laser fluence value of 0.1 J/cm^2 , with the corresponding 4 MW/cm^2 irradiance, remains below the plasma ignition threshold of CdSe. Indeed, as can be observed in the AFM and optical microscopy images, a higher amount of material were transferred and immobilized at 0.1 J/cm^2 laser fluence as compared to 0.2 J/cm^2 , and the fluorescence patterns are more intense. Besides, at 0.1 J/cm^2 laser fluence the fluorescence pattern reproduces the specific networklike surface morphology visible in Figure 8c. These results confirm that the CdSe/ZnS core–shell QDs were transferred at 0.1 J/cm^2 incident laser

fluence to the substrate surface without damage or selective evaporation.

■ CONCLUSION

The synthesized CdSe/ZnS core–shell QDs have a narrow size distribution, with dimensions between 4 and 6 nm. The obtained CdSe/ZnS QDs were immobilized by UV-MAPLE onto SiO_2 glass substrates covered by silica films. The formation of a specific self-organized network-like morphology was observed, built from micrometer-sized lines of CdSe/ZnS core–shell QDs. At high laser fluence value damage of QDs situated in the outmost surface layer of the frozen composite target can explain the reduced fluorescence of the processed and transferred material. At lower incident laser fluence the deposited QDs

structure the fluorescence pattern is more intense and reproduces the specific network-like surface morphology, proving that laser techniques are suitable for the immobilization of CdSe/ZnS QDs. The preserved functional properties make the immobilized QDs suitable for key applications as biosensors, lasers, or high performance electronic devices.

■ AUTHOR INFORMATION

Corresponding Author

*Phone: +34 93 581 37 25. Fax: +34 93 581 37 17. E-mail: egorgy@cin2.es.

■ ACKNOWLEDGMENT

The authors acknowledge the financial support from the Spanish National Research Council under the Contract Nos. 200860I211 and 200960I015, the Spanish Ministry of Science and Innovation for the PTA2008-1108-I contract, the Portugal-Spanish Bilateral Agreement No. 2007PT0007, and the Romanian National University Research Council under the Contract IDEAS No. 652.

■ REFERENCES

- (1) Du, K.; Ernst, F.; Pelsozy, M. C.; Barthel, J.; Tillmann, K. *Acta Mater.* **2010**, *58*, 836.
- (2) Ayyub, P. J. *Cluster Sci.* **2009**, *20*, 429.
- (3) Shen, L.; Zhang, H.; Guo, S. *Mater. Chem. Phys.* **2009**, *114*, 580.
- (4) Klimov, V. I. *J. Phys. Chem. B* **2006**, *110*, 16827.
- (5) Sun, C. Q.; Chen, T. P.; Tay, B. K.; Li, S.; Huang, H.; Zhang, Y. B.; Pan, L. K.; Lan, S. P.; Sun, X. W. *J. Phys. D* **2001**, *34*, 3470.
- (6) Jasleniak, J.; Smith, L.; van der Embden, J.; Mulvaney, P. *J. Phys. Chem. C* **2009**, *113*, 19468.
- (7) Feng, M.; Cundiff, S. T.; Mirin, R. P.; Silverman, K. L. *IEEE J. Quantum Electron.* **2010**, *46*, 951.
- (8) Kamat, P. V. *J. Phys. Chem. C* **2008**, *112*, 18737.
- (9) Reiss, P.; Protière, M.; Li, L. *Small* **2009**, *5*, 154.
- (10) Ziegler, J.; Merkulov, A.; Grabolle, M.; Resch-Genger, U.; Nanni, T. *Langmuir* **2007**, *23*, 7751.
- (11) Dabbousi, B. O.; Rodriguez-Viejo, J.; Mikulec, F. V.; Heine, J. R.; Mattoussi, H.; Ober, R.; Jensen, K. F.; Bawendi, M. G. *J. Phys. Chem. B* **1997**, *101*, 9463.
- (12) Zhu, C. Q.; Wang, P.; Wang, X.; Li, Y. *Nanoscale Res. Lett.* **2008**, *3*, 213.
- (13) Smith, A. M.; Mohs, A. M.; Nie, S. *Nat. Nanotechnol.* **2009**, *4*, 56.
- (14) Alivisatos, A. P. *Nat. Biotechnol.* **2004**, *22*, 47.
- (15) Riegler, J.; Ditengou, F.; Palme, K.; Nann, T. *J. Nanobiotechnol.* **2008**, *6*, 7.
- (16) Nizamoglu, S.; Demir, H. V. *J. Appl. Phys.* **2009**, *105*, 083112.
- (17) Gopal, A.; Hoshino, K.; Kim, S.; Zhang, X. *Nanotechnology* **2009**, *20*, 235201.
- (18) Kazes, M.; Saraidarov, T.; Reisfeld, R.; Banin, U. *Adv. Mater.* **2009**, *21*, 1716.
- (19) Klimov, V. I.; Mihailovsky, A. A.; McBranch, D. W.; Bawendi, M. G. *Science* **2000**, *287*, 1011.
- (20) Mihailovsky, A. A.; Malko, A. V.; Hollingsworth, J. A.; Bawendi, M. G.; Klimov, V. I. *Science* **2000**, *90*, 314.
- (21) Smirnova, T. N.; Sakhno, O. V.; Yezhov, P. V.; Kotlych, L. M.; Goldenberg, L. M.; Stumpe, J. *Nanotechnology* **2009**, *20*, 245707.
- (22) Wu, P. K.; Ringisen, B. R.; Krizman, D. B.; Frondoza, C. G.; Brooks, M.; Bubb, D. M.; Auyeung, R. C. Y.; Piqué, A.; Spargo, B.; McGill, R. A.; Chrisey, D. B. *Rev. Sci. Instrum.* **2003**, *74*, 2546.
- (23) Caricato, A. P.; Luches, A.; Rella, R. *Sensors* **2009**, *9*, 2682.
- (24) Hunter, C. N.; Check, M. H.; Bultman, J. E.; Voevodin, A. A. *Surf. Coat. Technol.* **2008**, *203*, 300.
- (25) Pate, R.; Lantz, K. R.; Stiff-Roberts, A. D. *Thin Solid Films* **2009**, *517*, 6798.
- (26) Aldana, J.; Wang, Y. A.; Peng, X. *J. Am. Chem. Soc.* **2001**, *123*, 8844.
- (27) Xie, R.; Kolb, U.; Li, J.; Basche, T.; Mews, A. *J. Am. Chem. Soc.* **2005**, *127*, 7480.
- (28) McDonagh, C.; Bowe, P.; Mongey, K.; MacCraith, B. D. *J. Non-Cryst. Solids* **2002**, *306*, 138.
- (29) Yu, S.; Wong, T. K. S.; Hu, X.; Pita, K. *J. Electrochem. Soc.* **2003**, *150*, F116.
- (30) Williams, A. T. R.; Winfield, S. A.; Miller, J. N. *Analyst* **1983**, *108*, 1067.
- (31) Baranov, A.; Rakovich, Y.; Donegan, J.; Perova, T.; Moore, R.; Talapin, D.; Rogach, A.; Masumoto, Y.; Nabiev, I. *Phys. Rev. B* **2003**, *68*, 165306.
- (32) Gao, X.; Nie, S. *J. Phys. Chem. B* **2003**, *107*, 11575.
- (33) Gallardo, I.; Hoffmann, K.; Keto, J. W. *Appl. Phys. A Mater. Sci. Process* **2009**, *94*, 65.
- (34) Sands, D.; Key, P.; Hoyland, J. *Appl. Surf. Sci.* **1999**, *138–139*, 240.
- (35) Mastio, E. A.; Fogarassy, E.; Cranton, W. M.; Thomas, C. B. *Appl. Surf. Sci.* **2000**, *154*, 35.
- (36) Sands, D.; Wagner, F. X.; Key, P. H. *J. Appl. Phys.* **1999**, *85*, 3855.